ELSEVIER

Polymer 41 (2000) 8579–8586

polymer

www.elsevier.nl/locate/polymer

Novel phosphorus-containing epoxy resins. Part II: curing kinetics

Chun Shan Wang*, Ching Hsuan Lin

Department of Chemical Engineering, National Cheng Kung University, Tainan 701, Taiwan, ROC

Received 16 August 1999; received in revised form 12 October 1999; accepted 14 January 2000

Abstract

Curing kinetics of glycidyl ether of cresol formaldehyde novolac or novel phosphorus-containing epoxy cured with diaminodiphenyl sulfone (DDS) were studied by the dynamic differential scanning calorimetry (DSC) and isothermal DSC method. Parameters of dynamic curing kinetic were calculated by using the Kissinger and Ozawa's methods, respectively. Parameters including k_1, k_2, m and n of isothermal curing kinetics were determined by an autocatalytic mechanism proposed by Kamal. The model gave a good description of curing kinetics up to the onset of vitrification. The effect of the diffusion control was described by an approach based on simple equations proposed by Chern and Poehlein. The relations concerning the activation energy of curing and structure of epoxy resins were discussed.

Keywords: Phosphorus; Differential scanning calorimetry; Epoxy

1. Introduction

Kinetic characterization of thermoset resins is fundamental in understanding structure/property/processing relationships for manufacturing and utilization of high performance composites. Curing kinetics models are generally developed by analyzing experimental results obtained by differential scanning calorimetry (DSC) [1–4]. DSC, both in the isothermal and dynamic modes, has been used extensively, assuming a proportionality between the heat evolved during the cure and the extent of reaction. In our previous paper [5], two multifunctional phosphorus-containing epoxy resins ($C_{12}P_2$ and $C_{12}P_4$, with phosphorus content 2 and 4%, respectively) were synthesized from the addition reaction of 9,10-dihydro-9-oxa-10-phosphaphenanthrene 10-oxide (DOPO) and the glycidyl ether of cresol formaldehyde novolac (functionality = 12, C_{12}) (Scheme 1). After curing with 4,4′-diaminodiphenyl sulfone (DDS), phenol novolac (PN) or dicyandiamide (DICY), they exhibited high glass transition and good flame-retardancy. For example: if phosphorus content of uncured epoxy resins is 2% (meet the criterion of flame-retardancy, UL-94 V-0 grade), T_g (measured by dynamic mechanical analysis) is 228°C for the DDS curing system; T_g = 178°C for the PN curing system and T_g = 213°C for the DICY curing system. Glass transition temperatures of these halogen-free epoxy resins are extremely high compared with common epoxy resins used for FR-4 laminates (T_g = 120–140°C).

Since curing kinetics, curing rate, variation of rate at various temperatures, activation energy of curing and other kinetic data provided information for the curing cycles of epoxies, which will ensure that the adequately cured epoxy is able to meet the requirements of its end use, the curing kinetics of C_{12}/DDS, $C_{12}P_2$/DDS and $C_{12}P_4$/DDS were studied by DSC using dynamic and isothermal experiments.

2. Experimental

2.1. Materials

4,4′-diaminodiphenyl sulfone (DDS) and 4,4′-diaminodiphenyl methane (DDM) were purchased from Acros. Multifunctional phosphorus-containing epoxy resins ($C_{12}P_2$ and $C_{12}P_4$, with phosphorus content 2 and 4%, respectively) were synthesized according our previous paper [1]. Glycidyl ether of cresol formaldehyde novolac (functionality = 12, C_{12}) with EEW 205 g/eq was supplied kindly by Nan Ya Plastics in Republic of China (trade name NPCN-704).

2.2. Characterization

DSC measurements were performed with a Perkin–Elmer DSC 7 supported by a Perkin–Elmer Computer for data

* Corresponding author. Tel.: +886-6-260-8219; fax: +886-6-234-4496.
E-mail address: cswang@mail.ncku.ed.utw (C.S. Wang).

0032-3861/00/$ - see front matter
PII: S0032-3861(00)00211-1

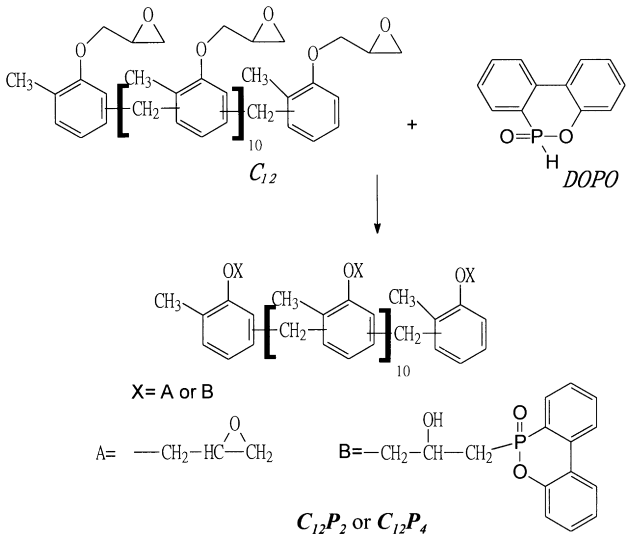

Scheme 1.

acquisition. The DSC was calibrated with high purity In and Zn. DSC dynamic data were obtained with 8 mg samples in a nitrogen atmosphere at a heating rate of 5–20°C/min using a Perkin–Elmer DSC 7. Isothermal cure reaction was conducted at various temperatures. The reaction was considered complete when the isothermal DSC thermogram leveled off to the baseline. The total area under the exothermic curve, which was based on the extrapolated baseline at the end of the reaction, was used to calculate the isothermal heat of cure, ΔH_0. After the cure reaction was completed in the calorimeter, the sample was cooled to 40°C. To determine the residual heat of reaction, ΔH_R, the samples after curing were scanned at 10°C/min from 40 to 300°C. The sum of the isothermal heat (ΔH_0) and residual heat of the reaction (ΔH_R) was taken to represent the total heat of cure (ΔH_T). The isothermal conversion at time t was defined as $\alpha(t) = \Delta H_0/\Delta H_T$.

3. Results and discussion

3.1. Curing behaviors

Fig. 1 showed heating scans (10°C/min) of C_{12}, $C_{12}P_2$, $C_{12}P_4$ cured with DDS and DDM, respectively. For the DDM curing system, the melting transition at about 90°C is the melting of DDM and the exothermic temperatures ranged from 100 to 220°C. For the DDS curing system exothermic transitions at about 160–300°C were observed. The exothermic temperature increased in the following order: DDM < DDS. Generally speaking, a curing agent exhibiting a lower exothermic temperature under the same set of curing conditions is more reactive toward the epoxy resins. It is therefore reasonable to propose that the chemical reactivity of these two curing agents toward the epoxy resin is as follows: DDS < DDM. The sulfone group in DDS is a

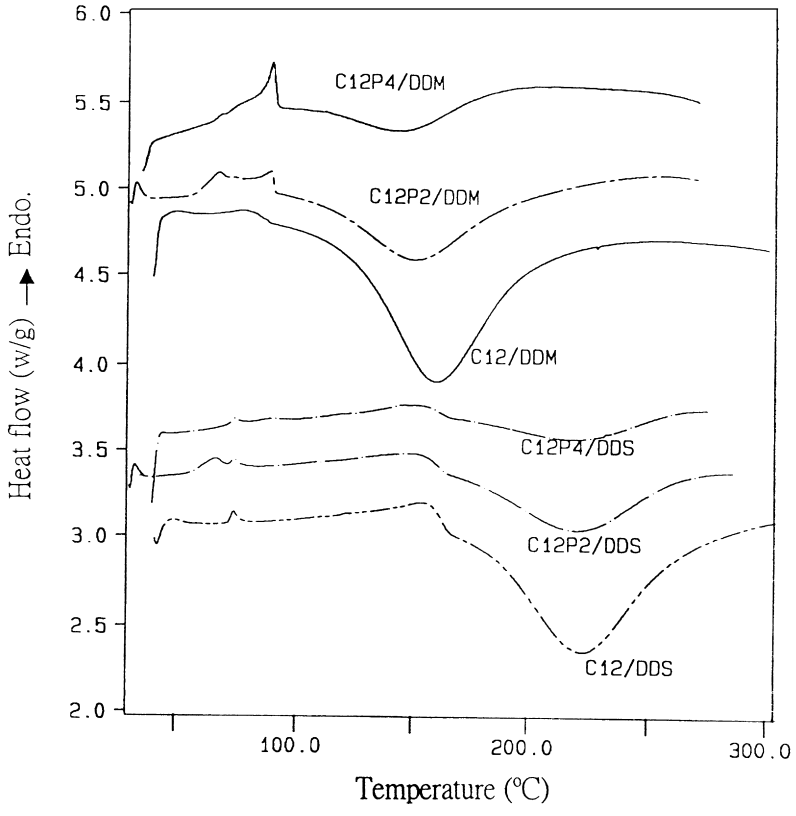

Fig. 1. DSC heating scans of C_{12}, $C_{12}P_2$, $C_{12}P_4$ cured with DDS and DDM at a heating rate of 10°C/min.

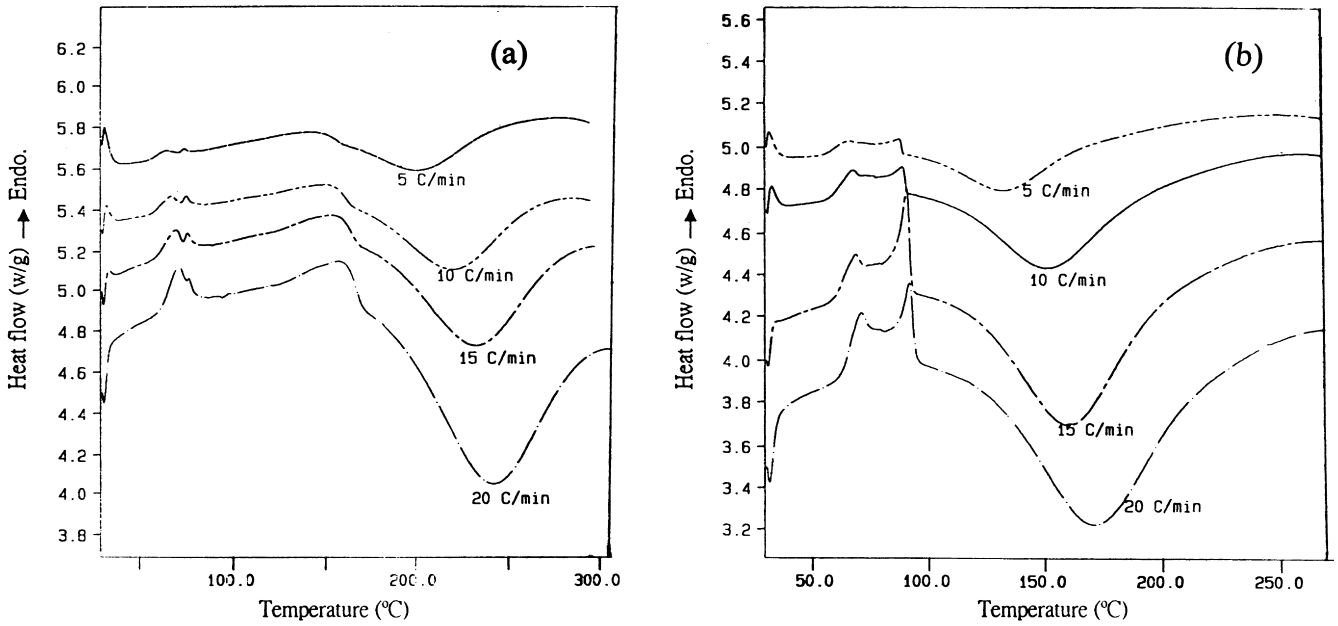

Fig. 2. DSC traces of: (a) $C_{12}P_2$/DDS; and (b) $C_{12}P_2$/DDM at various heating rates (5, 10, 15 and 20°C/min).

strong electronic withdrawing group both by negative induction (−I) and negative mesomeric (−M) effects. Thus, its nucleaphilicity is considerably reduced. DDM, without the mesomeric effect but with the positive induction effect of thr methylene group, therefore, has higher reactivity than that of DDS. Furthermore, the order of curing enthalpy was C_{12} series > $C_{12}P_2$ series > $C_{12}P_4$ series, which was reasonable due to the functionality C_{12} > $C_{12}P_2$ > $C_{12}P_4$, that is, the epoxy equivalent weight was C_{12} (205 g/eq) < $C_{12}P_2$ (276 g/eq) < $C_{12}P_4$ (485 g/eq). Besides, an interesting phenomenon was observed: curing exothermic peak temperatures were in the order of C_{12} series > $C_{12}P_2$ series > $C_{12}P_4$ series. Before explaining this phenomenon, the activation energy of curing reaction must be measured.

3.2. Curing kinetics

The activation energy of the curing reaction can be obtained by dynamic DSC scans or isothermal experiments. For a dynamic scan, the activation energy can be obtained by scanning the C_{12}/DDS, $C_{12}P_2$/DDS, $C_{12}P_4$/DDS system or C_{12}/DDM, $C_{12}P_2$/DDM, $C_{12}P_4$/DDM system at various heating rates. Two examples of the DSC heating traces ($C_{12}P_2$/DDS and $C_{12}P_2$/DDM) at various heating rates (5, 10, 15 and 20°C/min) were shown in Fig. 2(a) and (b). From the heating rate (β) versus reciprocal exothermic peak temperatures ($1/T_p$), the activation can be calculated by the following two methods, namely, Kissinger's [6] and Ozawa's method [7].

3.3. Dynamic method I (Kissinger's method [6])

The data from dynamic DSC measurements are analyzed by Eq. (1)

Since $T = T_0 + \beta t$, $\quad dT = \beta\, dt$

$$r = \frac{d\alpha}{dt} = \beta\frac{d\alpha}{dT} = Ae^{-\frac{E}{RT}}(1-\alpha)^n \tag{1}$$

where T is the temperature, T_0 the reference temperature, t the heating time, α conversion and β the heating rate. Since the maximum rate takes place when dr/dt is zero, differential equation of (1) with respect to time and equating the resulted expression with zero gives the following equation:

$$\beta\frac{E}{RT_p^2} = An(1-\alpha)p^{n-1}e^{\frac{-E}{RT_p}} \tag{2}$$

where T_p is the peak temperature of the DSC exothermic curves and it is also the temperature where the maximum reaction occurs. Eq. (2) can be written in the natural logarithm form shown as follows:

$$-\ln\left(\frac{\beta}{T_p^2}\right) = \ln\left(\frac{E}{R}\right) - \ln(An) - (n-1)\ln(1-\alpha)_p + \frac{E}{RT_p} \tag{3}$$

If plots of $-\ln(\beta/T_p^2)$ against $(1/T_p)$ is linear, the activation energy can be obtained from the slope of the corresponding straight line. Fig. 3(a) and (b) are the plots of $-\ln(\beta/T_p^2)$ against $(1/T_p)$ for the DDS curing system and the DDM curing system, respectively, and they are all linear. The activation energy calculated from Fig. 3(a) for C_{12}/DDS, $C_{12}P_2$/DDS and $C_{12}P_4$/DDS is 66.1, 63.9 and 52.6 kJ/mol and calculated from Fig. 3(b) for C_{12}/DDM, $C_{12}P_2$/DDM and $C_{12}P_4$/DDM is 48.5, 46.6 and 44.3 kJ/mol, respectively. The fact that the activation energy decreased

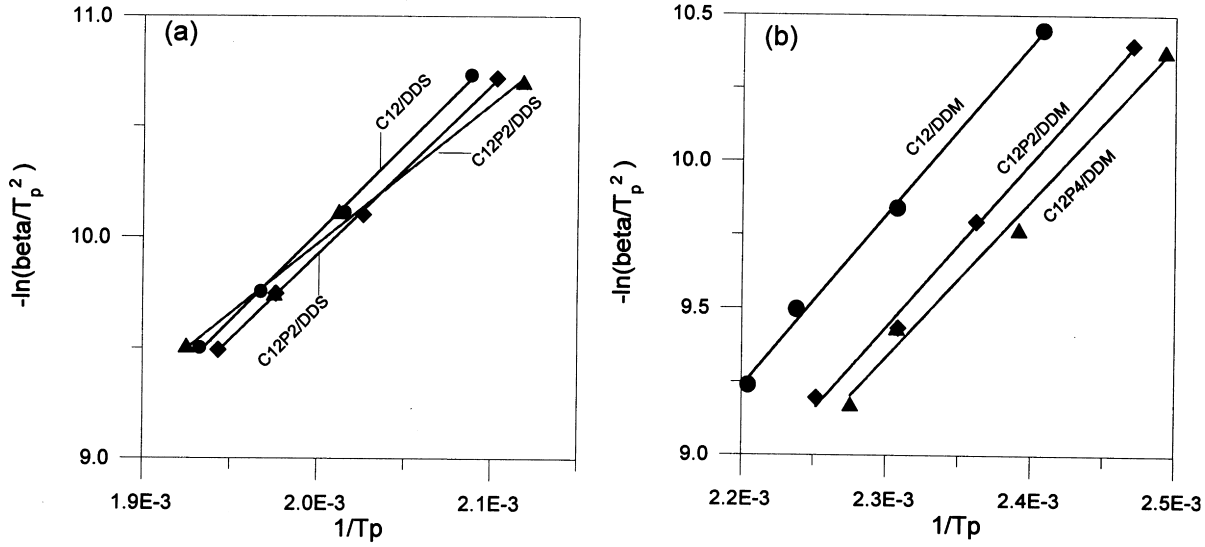

Fig. 3. Plots of $-\ln(\beta/T_p^2)$ against $(1/T_p)$ for: (a) DDS curing system; and (b) DDM curing system.

with the phosphorus content was consistent with the result that the order of curing exothermic peak temperature was in the order of C_{12} series > $C_{12}P_2$ series > $C_{12}P_4$ series.

3.4. Dynamic method II (Ozawa's method [7])

Another theoretical treatment, namely, the Ozawa's method can also be applied to the thermal data. He reported Eq. (4)

$$\log \beta = \frac{1}{2.303}\ln \beta = -0.4567\frac{E}{RT} + \left(\log\frac{AE}{R} - \log F(\alpha) - 2.315\right) \quad (4)$$

where β is the heating rate, E the activation energy, R the ideal gas constant and $F(\alpha)$ the conversion dependent term.

Thus, at the same conversion, a plot of ln (β) versus $1/T_p$ (Fig. 4(a) and (b)) should be a straight line with a slope of $1.052 \times E/R$. The activation energy calculated from Fig. 4(a) for C_{12}/DDS, $C_{12}P_2$/DDS and $C_{12}P_4$/DDS was 70.7, 68.5 and 57.8 kJ/mol and calculated from Fig. 4(b) for C_{12}/DDM, $C_{12}P_2$/DDM, and $C_{12}P_4$/DDM was 53.0, 51.0 and 48.7 kJ/mol, respectively. The fact that the activation energy decreased with the phosphorus content was also consistent with the result of Figs. 1 and 3.

Compared with C_{12}, the preformed hydroxyl groups of $C_{12}P_2$ or $C_{12}P_4$ derived from the addition reaction of DOPO and oxirane ring (see Scheme 1) will form hydrogen bonding with oxirane ring and thus enhance the curing reaction. The enhancement of curing was also observed in the PC/epoxy system [8]. Thus, the activation energy decrease in the order of $C_{12}P_2$ system < $C_{12}P_2$ system < C_{12} system. This can be further confirmed by isothermal curing kinetics discussed below.

3.5. Isothermal curing kinetics

Fig. 5(a) and (b) showed the $d\alpha/dt$ versus time of C_{12}/DDS and $C_{12}P_2$/DDS at various temperatures. It was seen that the reaction rate was affected by the isothermal curing temperature and the reaction time. At a given temperature, the reaction rate increased with conversion initially and passed through a maximum, and then gradually slowed down, finally tending to zero. Additionally, at a given time, a higher isothermal curing temperature gained a higher reaction rate. Moreover, the higher the isothermal temperature, the shorter the reaction time to complete the curing reaction. Fig. 6 showed that the reaction rate of the system reaches a maximum at time $t > 0$, which was characteristic of the autocatalytic reaction. Fig. 6(a) and (b) showed plots of $d\alpha/dt$ against conversion for C_{12}/DDS and $C_{12}P_2$/DDS at various curing temperatures, respectively. The maximum reaction rates occurred at conversion > 0, which is also characteristic for the autocatalytic reaction. Thus, the autocatalytic character is not changed for the phosphorus-containing epoxy ($C_{12}P_2$) and the kinetic model is appropriate to describe the isothermal behavior of the system.

Generally, most amine-cured epoxy systems are expressed as follows [9]:

$$d\alpha/dt = (k_1 + k_2\alpha^m)(1-\alpha)^n \quad (5)$$

where α is the conversion, k_1 and k_2 the apparent rate constants, and m and n the kinetic exponents of the reactions. To compute parameters of Eq. (5), several methods have been proposed in the literature [10–12], in many of them it was assumed that the total reaction order was 2, $m + n = 2$, restraining the range of application of the proposed model. In the present study, parameters m, n, k_1 and k_2 were estimated without any constraints on them by fitting the experimental data by graphical method and non-linear curve fitting. The graphical method was described as

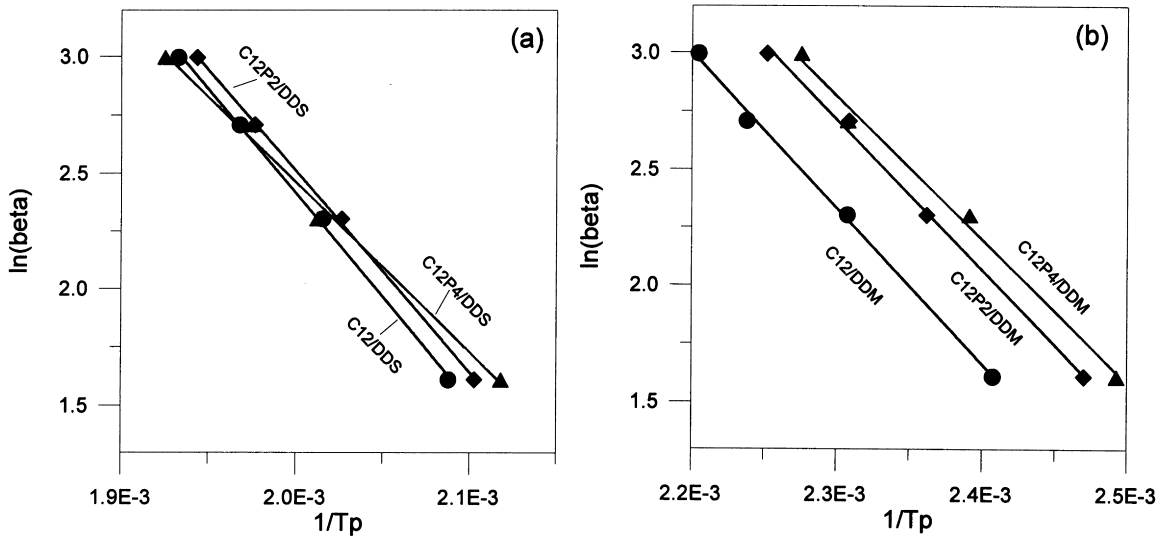

Fig. 4. Plots of ln (β) versus $1/T_p$ for: (a) DDS curing system; and (b) DDM curing system.

follows: the constant k_1 in equation can be calculated from the initial reaction rate at $\alpha = 0$. The kinetic constants are assumed to be of the Arrhenius form $k_1 = A_1 \exp(-E_1/RT)$ and $k_2 = A_2 \exp(-E_2/RT)$, where A_1, A_2 are the pre-exponential constants, E_1, E_2 the activation energies, R the gas constant and T the absolute temperature. Eq. (5) is rewritten in the following form:

$$\ln(d\alpha/dt) = \ln(k_1 + k_2\alpha^m) + n\ln(1-\alpha) \quad (6)$$

Except for the initial region, a plot of $\ln(d\alpha/dt)$ versus $\ln(1-\alpha)$ is expected to be linear with a slope n. Eq. (6) can then be further rearranged to give

$$\ln\{[d\alpha/dt)/(1-\alpha)^n] - k_1\} = \ln k_2 + m\ln\alpha \quad (7)$$

The first term of Eq. (7) can be computed from the previously estimated values of k_1 and n. If the left term of Eq. (7) is plotted against $\ln(\alpha)$, a straight line is yielded whose slope and intercept allow the estimation of m, and kinetic constant, k_2, respectively. Preliminary kinetic parameters can be obtained on the first trial. The kinetic parameters, k_2, m and n can be estimated from the stated procedures. To obtain more precise values the iterative procedure should be utilized. The equation can be further rearranged to give the following form:

$$\ln(d\alpha/dt) - \ln(k_1 + k_2\alpha^m) = n\ln(1-\alpha) \quad (8)$$

The left terms of the above equation can be plotted against $\ln(1-\alpha)$. A new value of the reaction order n can be obtained from the slope. The same iterative procedure repeated until apparent convergence of m and n values.

The plots of the left terms in Eq. (7) versus ln α for C_{12}/DDS and $C_{12}P_2$/DDS at various temperatures were shown in Fig. 7(a) and (b). Fig. 7 exhibited linearity before the reaction became diffusion-controlled (discussed below). From

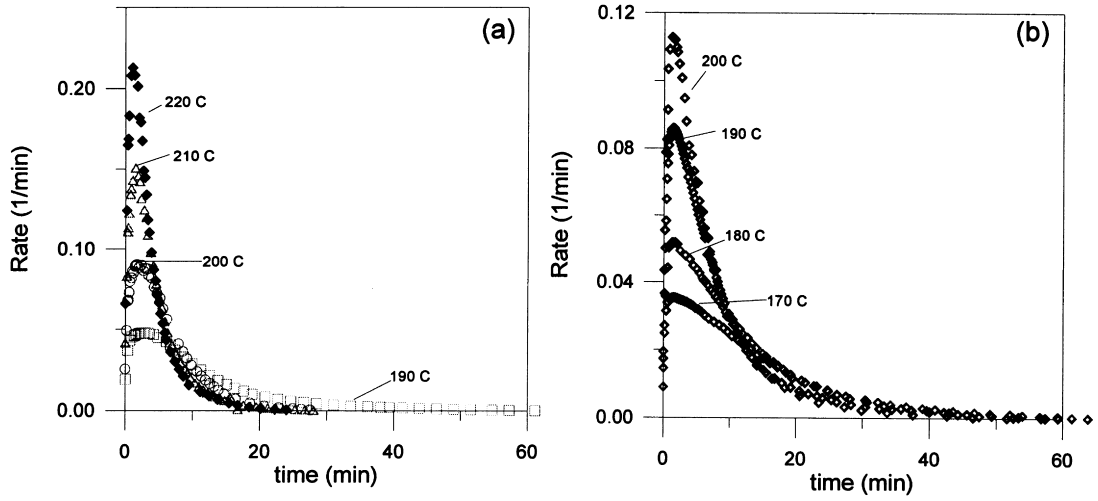

Fig. 5. Plots of $d\alpha/dt$ versus time of: (a) C_{12}/DDS; and (b) $C_{12}P_2$/DDS at various temperatures.

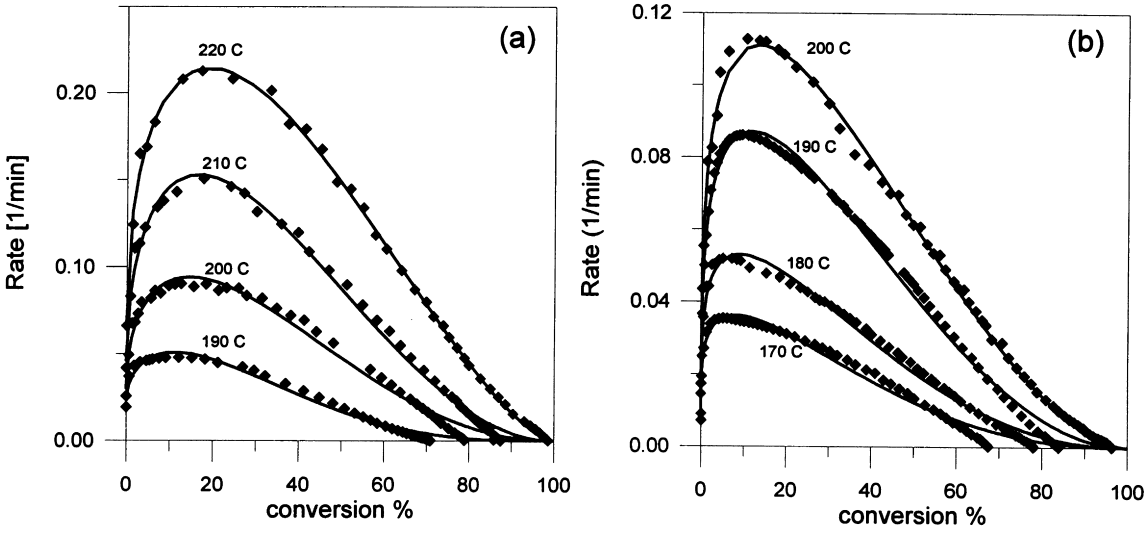

Fig. 6. Plots of $d\alpha/dt$ against conversion for: (a) C_{12}/DDS; and (b) $C_{12}P_2$/DDS at various curing temperatures. The data points were experimental data and the solid lines were plotted according to the autacatalytic model.

the slope and intercept, m and k_2 was obtained. Parameters of autocatalytic model, k_1, k_2, m and n, calculated from above discussion for each curing temperature were shown in Table 1. According to the rate constant k_1 and k_2, the Arrhenius plots were shown in Fig. 8, which yields the value of 65.7, 41.5 and 66.2, 74.3 kJ/mol for the associated activation energies (E_1 and E_2) of C_{12}/DDS and $C_{12}P_2$/DDS, respectively. In an ideal condition, a successful model should well describe the experimental data throughout the whole range of cure. But in this work, diffusion and the etherification reaction were not taken into account in the kinetic model. In order to demonstrate the curing behavior described by Kamal's equation, it was necessary to compare the results from model prediction with the experimental data. The solid lines in Fig. 7 were plotted by the autocatalytic model using parameters shown in Table 1. The model fitted the experimental data quite well in the early stage of the curing. However, deviations were observed in the later stage, which was attributed to the effect of diffusion control. As the cure proceeds and the resin crosslinked, the glass transition temperature of the curing resin increased. For cure temperatures well above T_g, the rate of reaction between the epoxy and the reactive groups of hardener was chemical kinetically controlled. When T_g approached the curing temperature, the resin passed from a rubbery state to a glassy state and the curing reactions became diffusion controlled, and eventually became very slow and finally stopped. This accounts for the fact that the experimental conversion and reaction rates were lower than those predicted by the autocatalytic kinetic model.

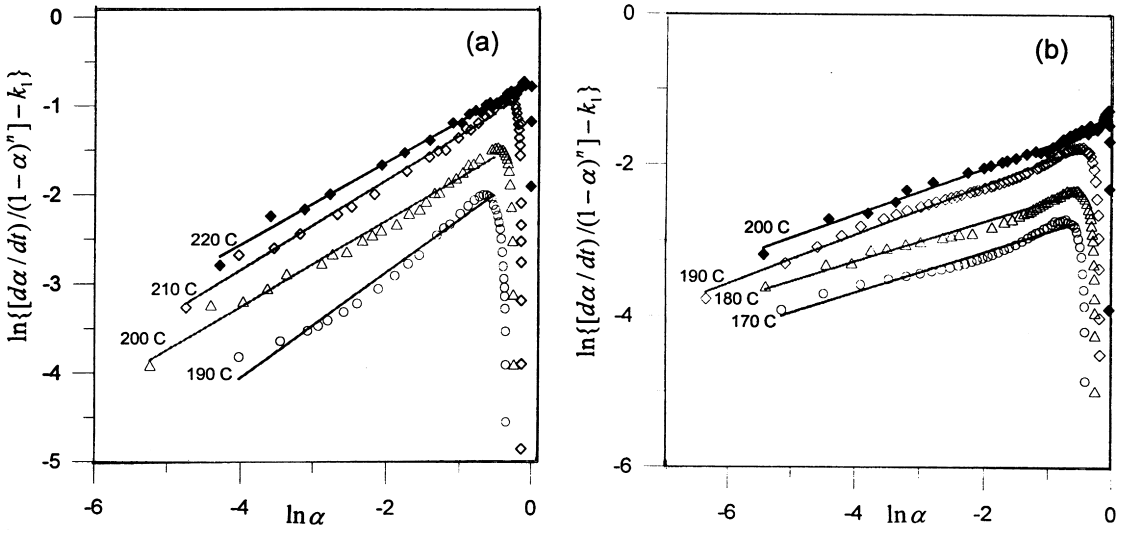

Fig. 7. Plots of left term in Eq. (7) versus ln α for: (a) C_{12}/DDS; and (b) $C_{12}P_2$/DDS at various temperatures.

Table 1
Values of m, n, k_1, k_2, α_c and C estimated at different temperatures

Temperature (°C)	m	n	$k_1 \times 10^3$	$k_2 \times 10^3$	E_1 (kJ/mol)	E_2 (kJ/mol)	ln A_1	ln A_2	α_c	C
C_{12}/DDS										
220	0.46	1.51	65.4	490.3					0.98	42
210	0.51	2.01	46.0	434.4	65.7	66.2	13.3	15.5	0.85	70
200	0.48	2.18	29.9	260.6					0.76	55
190	0.57	3.04	23.5	174.0					0.67	44
$C_{12}P_2$/DDS										
200	0.30	1.74	14.5	234.3					0.97	17
190	0.31	1.99	13.8	188.6	41.5	74.3	6.4	17.5	0.81	25
180	0.25	2.21	8.9	103.8					0.74	32
170	0.25	2.41	7.6	69.2					0.64	50

Chern and Poehlein [13] proposed a semiempirical relationship based on free volume considerations to explain the diffusion control in cure reactions. When the degree of cure reaches a certain critical value α_c, diffusion control takes over and the diffusion-controlled rate constant K_d is given by

$$K_d = K_c \exp[-C(\alpha - \alpha_c)] \quad (9)$$

where K_c is the rate constant for non-diffusion-controlled (chemical) kinetics and C a constant. According to Rabinowitch [14], the overall effective rate constant K_e can be

$$1/K_e = 1/K_d + 1/K_c \quad (10)$$

expressed in terms of K_d and K_c as follows:

Combining Eqs. (9) and (10), one can define a diffusion factor $f(\alpha)$ by

$$f(\alpha) = K_e/K_d = \frac{1}{1 + \exp[C(\alpha - \alpha_c)]} \quad (11)$$

with C and α_c, the critical conversion, being two empirical parameters. The effective reaction rate was equal to the chemical reaction rate multiplied by this factor, $f(\alpha)$. When values of α is significantly lower than α_c, $f(\alpha)$ is approximately equal to 1 and diffusion control is negligible. When α approaches α_c, $f(\alpha)$ began to decrease, reaching 0.5 when $\alpha = \alpha_c$. Beyond this point it continued to decrease, eventually approaching zero, so that the reaction became very slow and eventually stopped. In this work, data for $f(\alpha)$ were obtained by dividing the experimental values of $d\alpha/dt$ by those predicted by the autocatalytic kinetic model. Values of α_c and C obtained by fitting $f(\alpha)$ versus α are shown in Table 1. An increase in α_c when an increasing temperature was observed, but for the coefficient C, no discernible trend was found, in agreement with the studies of Cole et al. [15] and Barral et al. [16] on epoxy–amine systems.

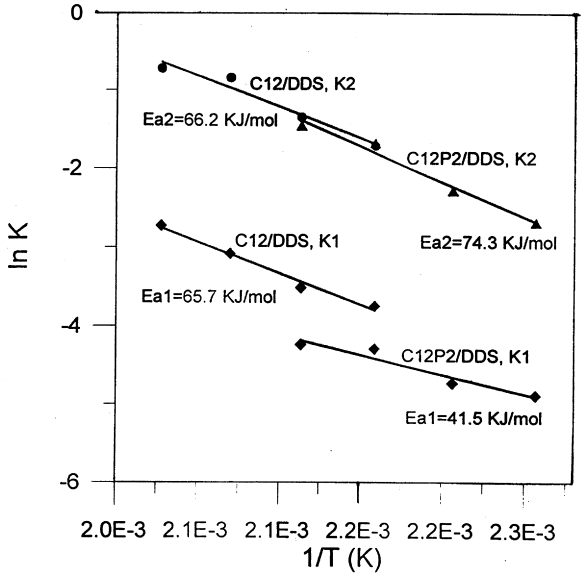

Fig. 8. Arrhenius plots of rate constants k_1 and k_2.

4. Conclusion

According to Kissinger and Ozawa's methods, the dynamic curing kinetics of C_{12}/DDS, $C_{12}P_2$/DDS, $C_{12}P_4$/DDS were studied. The activation energy of curing decreased in the order of $C_{12}P_4$ system < $C_{12}P_2$ system < C_{12} system. This can be explained by the fact that the preformed hydroxyl group in $C_{12}P_2$ or $C_{12}P_4$ may form a hydrogen bond with the oxirane ring and thus enhanced the curing reaction. C_{12}/DDS and $C_{12}P_2$/DDS were also studied by the autocatalystic model proposed by Kamal. The model gave a good description before diffusion-control. When diffusion control took place, the curing kinetics can be described by Chern and Poehlein's method. From Arrhenius plots, E_1 and E_2 were obtained. E_1, obtained from the Arrhenius plots, decreased in the order of $C_{12}P_2$/DDS < C_{12}/DDS, which was consistent with the activation obtained from dynamic curing.

Acknowledgements

Financial support of this work by the National Science Council of Republic of China is gratefully appreciated (NSC88-2214-E006-002).

References

[1] Guthner T, Hammer B. J Appl Polym Sci 1993;50:1453.
[2] Su CC, Woo EM. Polymer 1995;36:2883.
[3] Khanna U, Chanda M. J Appl Polym Sci 1993;49:319.
[4] Lin ST, Huang SK. J Appl Polym Sci 1996;62:1641.
[5] Wang CS, Lin CH. Submitted for publication.
[6] Kissinger HE. Anal Chem 1957;29:1072.
[7] Ozawa T. Bull Chem Soc Jpn 1965;38:1881.
[8] Lin ML, Chang KH, Chang FC, Li S, Ma CC. J Polym Sci, Polym Phys 1997;35:2169.
[9] Kamal MR. Polym Engng Sci 1974;14:23.
[10] Ryan ME, Dutta A. Polymer 1979;20:203.
[11] Kenny JM. J Appl Polym Sci 1994;51:761.
[12] Moroni A, Mijovic J, Pearce E, Foun C. J Appl Polym Sci 1986;32: 3761.
[13] Chern CS, Poehlein GW. Polym Engng Sci 1987;27:788.
[14] Rabinowitch E. Trans Faraday Soc 1937;33:1225.
[15] Cole KC, Hechler JJ, Noel D. Macromolecules 1991;24:3098.
[16] Barral L, Cano J, Lopez AJ, Lopez J, Nogueira P, Ramirez C. J Appl Polym Sci 1995;56:1029.